Predictive frequency-based sequence estimator for control of grid-tied converters under highly distorted conditions

Cristian Blanco*, Pablo García*, Ángel Navarro-Rodríguez*, and Mark Sumner†
*University of Oviedo. Dept.of Elec., Computer & System Engineering
Gijón, 33204, Spain
e-mail: blancocristian@uniovi.es, garciafpablo@uniovi.es, navarroangel@uniovi.es

†The University of Nottingham. Department of Electrical and Electronic Engineering
University Park, Nottingham. NG7 2RD, UK
e-mail: Mark.Sumner@nottingham.ac.uk

***Abstract*—This paper proposes a novel frequency-based predictive sequence extractor that allows to isolate the harmonic components of both voltages and currents needed for the control of grid-tied converters. The proposed method is based on a modification of the Sliding Goertzel Transformation (SGT) that allows to include a predictive behavior with a prediction horizon equal to the processing window needed for the algorithm. The technique performance is compared with the well-established DSOGI alternative, allowing for a higher bandwidth in the estimation as well as improved immunity to changes in the magnitude, frequency and phase of the tracked signals. Additionally, the impact of the proposed method on the closed-loop performance of the current controlled converter is proposed as a metric, thus enabling other researches to have a clear view about the expected real impact of the different existing methods.**

I. Introduction

Distributed power generation (DPG) is expected to play an important role in the short and medium term design of the generation, transport and distribution system. This is due to the penetration of renewable generation units that allows to produce power, providing at the same time ancillary services (harmonic compensation [1], magnitude and frequency restoration [2],...) An engaging characteristic of the DPG systems based in renewable generation is that they help to decrease the emissions since the DPG units are placed near the power is consumed. On the other hand, the use of DPG increases the complexity of the whole system due to the coexistence of several systems with different characteristics (nominal power, output impedance, workload, transient response ...)

DPG units are usually connected to the utility grid by using electronic power converters (mainly PWM voltage source inverters, VSI [3], [4]). VSI control strategies are mainly composed by an inner current control loop, an outer voltage control loop and an external power control loop [5] based, all of them in general, on proportional-integral (PI [3], [4]) or proportional-resonant (PRES [5]) controllers. To perform an accurate control of the fundamental component of the current, voltage or power, the use of PI and PRES controllers requires to estimate the magnitude, frequency and phase of the fundamental component of the utility grid. Furthermore, if a highly harmonic content is present on the grid, the estimation of frequency, phase and magnitude for additional harmonics is a desirable feature.

During last decades, several authors have been working on the development of synchronization techniques able to work under a wide range of working conditions. In this regard, the utility grid voltage may be polluted with harmonic components (due to the use of nonlinear loads) or unbalanced conditions (due to single-phase loads). At the same time, the utility grid magnitude and frequency may oscillate between values defined in the grid codes. Phase jumps could also occur while grid voltage measurements could be incorrect, especially in terms of DC components due to the voltage sensors [6]. The VSI control is required to be fast and accurate under all of these disturbances, the synchronization technique being a key point of the DPG control.

Synchronization techniques can be divided in open-loop [7], [8] or closed-loop [9]–[14]. Open-loop methods estimate the PCC voltage magnitude, frequency and phase without any feedback while closed-loop methods are based on locking one characteristic of the input signal, e.g. the frequency (frequency-locked-loop, FLL [9]) or phase (phase-locked-loop, PLL [11]). Nowadays, closed-loop techniques are preferred due to their better performance, a common concern being how to deal with grid disturbances that affect to the parameter estimation. The operation of closed-loop methods makes them to naturally adapt their magnitude and frequency estimations

The present work has been partially supported by the predoctoral grants program Severo Ochoa for the formation in research and university teaching of Principado de Asturias PCTI-FICYT under the grant ID BP14-135. This work also was supported in part by the Research, Technological Development and Innovation Program Oriented to the Society Challenges of the Spanish Ministry of Economy and Competitiveness under grant ENE2016-77919-R and by the European Union through ERFD Structural Funds (FEDER).

when these parameters deviate from their nominal values. Thus, research efforts have been traditionally focused in the development of techniques to remove the unwanted effects of additional harmonic components. One possible solution is to reduce the controller bandwidth of the closed-loop structure. However, this is at the price of a transient response degradation, which is not an acceptable solution in most cases. Alternatively, a filtering stage can be implemented, pre-filter and filter in the loop techniques being the most acceptable solutions [12].

A pre-filter stage feeds the closed-loop method with a filtered version of the grid voltage that contains only the fundamental component. DSOGI-FLL [9], MCCF-PLL [13], DSOGI-PLL [10], or CCCF-PLL [14] are examples of pre-filter stage methods. At the same time, filter on the loop techniques ([12], [15]) remove the unwanted effects of harmonics and unbalances inside the closed loop. In both cases, filters can be implemented by using second-order generalized integrators [9], [10], notch filters [12], complex-coefficient filters [13], [14], lead compensators [15] or moving average filters [16].

When using filtering stages, some aspects must be carefully taken into account: filters introduce phase delays that must be online estimated and compensated [17], transient response is affected [6], filters need to adapt their central frequency under frequency deviations [13] and magnitude and phase jumps affect to the frequency, magnitude and phase estimation [12].

In order to deal with these drawbacks, this paper proposes the use of the SGT [18] to estimate the fundamental and harmonic components of the utility grid. Predictive techniques are proposed to boost the Goertzel transient response while a wide frequency resolution is used to compute the algorithm, making the system frequency-adaptive. Experimental verification is provided to test the performance of the proposed method under several grid disturbances, including magnitude changes, frequency deviations, harmonic components and phase jumps.

This paper is organized as follows, in section II, the mathematical approach based on the sliding Goertzel algorithm is explained. Following, the proposed predictive algorithm is detailed, including simulation results to demonstrate its effectiveness. In II-A, the use of a fusion method for an estimation based both on the sliding implementation and on the predictive proposal is included. Section II-B describes the proposed method for the frequency estimation and the impact of frequency variation over the voltage magnitude and phase estimated values. In section III, the evaluation of the method using a programmable voltage supply is included. Finally, in IV, the obtained experimental results are included, thus validating the approach of the proposed method.

II. Implementation

The basics of the proposed method rely on an efficient implementation of the Discrete Fourier Transform (DFT) by using the recursive Goertzel implementation [19], valid for the extraction of harmonic components in real-time applications. The implementation has a lower computational burden when compared with traditional FFT-based approach for a low number of harmonics. Specifically, for calculating M harmonics from an input data vector of length N, the associated cost of the Goertzel algorithm can be expressed as $O(N, M)$, whereas for the FFT is $O(N, \log_2 N)$. Obviously, when the number of calculated harmonics meets $M \leq \log_2 N$, then the Goertzel approximation is the preferred choice. In this paper, one fundamental cycle, assuming a $50Hz$ nominal frequency, is considered at $10kHz$ sample rate, leading to a time window of $20ms$ and 200 samples. With the proposed parameters, the calculations using the Goertzel approach are faster than the FFT alternative when the calculated number of harmonics is $M \leq 8$. For the validation of the system, the harmonics detailed in Table I are used. The implementation is detailed in pseudo-code in Algorithm 1 and the corresponding block diagram is shown in Fig. 1. At the implementation, the h input variable contains the harmonic order of the sequences being analyzed.

TABLE I
Considered harmonics.

Harmonic Order	Mag (p.u.)
1	1
-5	0.2
7	0.2

Algorithm 1 Sequence extractor using Goertzel algorithm.

$f_{bin} \leftarrow 2\pi h/N$
$a_f \leftarrow 2\cos(f_{bin})$
$b_f \leftarrow e^{-jf_{bin}}$
$sk \leftarrow$ Initialize to zero
$k \leftarrow 1$, $k1 \leftarrow 2$, $k2 \leftarrow 3$
for $hh \leftarrow 1$,number of elements in f_{bin} (harmonics) **do**
  for $n \leftarrow 1, N-1$ **do**
    $sk(hh,k) = x(n) + a_f(hh) * sk(hh,k1) - sk(hh,k2)$
    $sk(hh,k2) = sk(hh,k1)$
    $sk(hh,k1) = sk(hh,k)$
  end for
  $sk(hh,k) = a_f(hh) * sk(hh,k1) - sk(hh,k2)$
  $y(hh,N) = (sk(hh,k) - sk(hh,k1) * b_f(hh))/N$
end for

An example of the evolution in time domain of the recursive Goertzel estimation, compared to the actual magnitudes of the harmonics is shown in Fig. 2. As it can be seen, when the input signal is at steady state during the $20ms$ needed for the completion of the algorithm, the estimation converges to the desired values. By looking at the represented graphs, two important conclusions can be obtained: 1) The estimation procedure is discontinuous, being the computed harmonic values restarted at each processing window. Obviously, this must be addressed for using the method for converter control application, as the one proposed in this paper. Often, overlapping is used for improving the situation (see Fig. 2c).

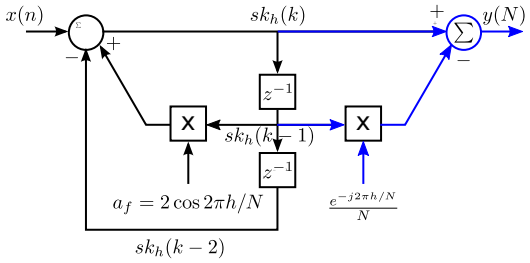

Fig. 1. IIR implementation of the Goertzel algorithm. Black traces are for the recursive part implementation. Blue traces represent the operations to be done at the last step ($k = N$).

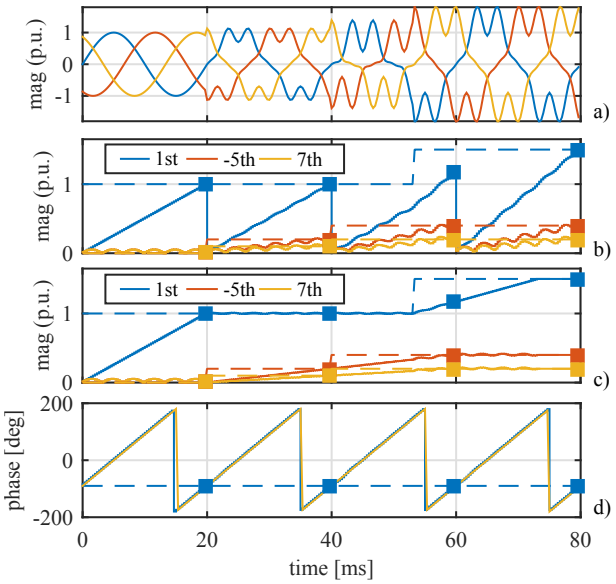

Fig. 2. Recursive Goertzel estimation for a three phase system with the harmonic contents shown in Table I. The dotted lines correspond to the real value of each of the harmonics. The square dots represent the estimated value at the end of each block. a) waveforms, b) and c) recursive Goertzel estimation with 0 and N-1 overlap, d) phase error.

However, this comes with an additional cost due to the number of operations required at each sample being multiplied by the number of overlapping samples. Alternatively, an efficient sliding approach of the algorithm (SGT) has been proposed for real-time signal processing applications, being the selected choice for our investigations [18]. 2) The estimated magnitude needs the total number of samples and time, $N = 200, t = 20ms$, to converge to the correct value. This would raise an unacceptable delay when the estimation is used as a feedback signal. However, it can be also seen that the evolution of the fundamental component (1^{st} harmonic) estimation is linear during the estimation window and barely affected by the harmonic content.

According to 2), this paper proposes to incorporate a predictive SGT implementation (P-SGT) that improves the convergence speed and, at the same time, avoids the extra calculations of the overlapping. The predictive behavior is implemented by a two-step algorithm. Firstly, a linear recursive least squares estimation (LSE) is run over the output of each

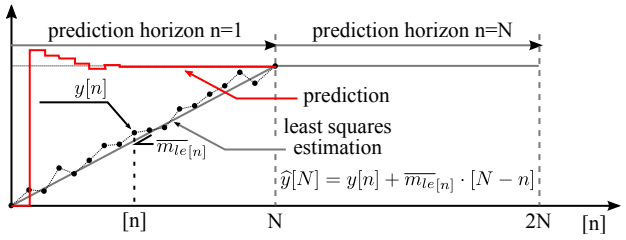

Fig. 3. Graphical representation of the proposed predictive algorithm. The slope at each of the points is filtered by a moving average filter for reducing the derivative noise.

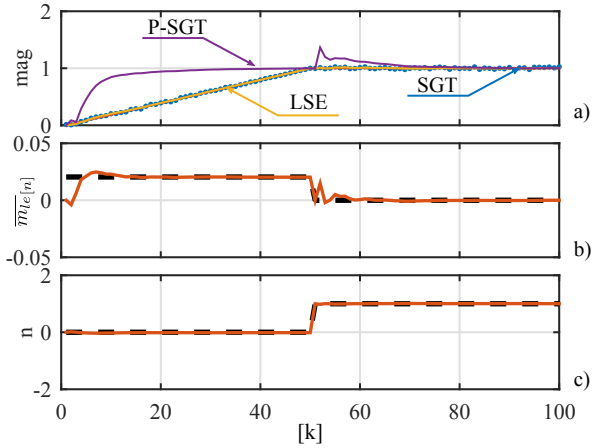

Fig. 4. Proposed P-SGT implementation. a) evolution of the magnitude. Actual samples are represented by blue dots, the output of the SGT by the red line and the prediction by the purple line. b) evolution of the predicted slope, c) evolution of the predicted offset. A window of $N = 50$ have been used for demonstration purposes.

sample of the SGT. This will lead to a linear representation of the corresponding datapoints. It must be remarked that being the output values of the SGT complex, two different least squares estimation can be obtained: one for the module and another one for the phase. Even considering this linear condition both for the magnitude and the phase estimation, at this paper the phase estimation is directly obtained from the Goertzel algorithm due to the fact that an accurate phase estimation can be obtained before each window is completed. Secondly, the module value at the end of each of the estimation windows is predicted. This last step is implemented at each step by again considering the linear evolution (1)

$$\widehat{y}[N] = y[n] + \overline{m_{le}}[n] \cdot [N - n] \tag{1}$$

, where $\overline{m_{le}}[n]$ is the moving average slope estimated by the LSE approach, N the window size and n the actual sample. A graphical description for the algorithm is shown in Fig. 3.

The simulation results with the proposed methods is shown in Fig. 4. As it can be seen, the results obtained by the P-SGT approximations notably improves the convergence speed of the estimation. However, even with the averaged slope calculation, some peak transients can be observed at the beginning of each processing window. This behavior is inherent to the involved derivative process. By comparing the smooth transitions using

the SGT, is is clear that both estimations can work in a complementary approach. For that reason, the final proposal for the estimation method will use a combination of both alternatives. The combined estimation will be based on the rate of change in the SGT estimation. As previously discussed, during the convergence time for the SGT, the estimation will exhibit a mostly linear change. On the contrary, once the estimation has reached the final value it will have a mostly zero variation. Based on that, the P-SGT will be favored during the transients, whereas the classical SGT will be mostly used at the steady state. Next section shows the mathematical formulation of the fusion algorithm as well as a numerical evaluation about the method performance.

A. Combined SGT and P-SGT estimation

Considering the performance of both the SGT and P-SGT strategies shown in Fig. 4,it is proposed to combine both methods, leading to the so called PF-SGT, for getting the final expression. For the fusion rule, an equation on the form (2) is proposed, where the value of the fusion gain ($k^f_{h\omega_e}$) is given by (3).

$$X^{pf-sgt}_{h\omega_e} = X^{p-sgt}_{h\omega_e} \cdot (1 - k^f_{h\omega_e}) + X^{sgt}_{h\omega_e} \cdot (k^f_{h\omega_e}) \quad (2)$$

$$k^f_{h\omega_e} = exp\left(-abs\left(\frac{mavg\left(\triangle X^{sgt}_{h\omega_e}\right)}{max\left(\triangle X^{sgt}_{h\omega_e}\right)}\right)\right)^{\cdot g_{h\omega_e}} \quad (3)$$

Where the presented variables are defined as follows:

- $X^{pf-sgt}_{h\omega_e}$. Estimation of harmonic component h at fundamental frequency ω_e for variable X using the PF-SGT method.
- $X^{p-sgt}_{h\omega_e}$. Estimation of harmonic component h at fundamental frequency ω_e for variable X using the P-SGT method.
- $X^{sgt}_{h\omega_e}$. Estimation of harmonic component h at fundamental frequency ω_e for variable X using the SGT method.
- $\triangle X^{sgt}_{h\omega_e}$ is the rate of change of the module of the estimated harmonic components by the SGT algorithm.
- $mavg$. Moving average function.
- max. Maximum variation function.
- $g_{h\omega_e}$. Gain of the exponential function used for tuning the fusion system.

Evolution of the estimation and the adaptive gain is shown in Fig. 5. As clearly shown, the fusion helps on removing the transient at the beginning of each of the processing windows. Ongoing work is being carried out for the selection of the optimal fusion gain.

B. Frequency estimation

When the proposed PF-SGT method is applied for the estimation of grid voltages and currents, variations at the frequency must be considered. As known, frequency domain methods based on the DFT assume the periodicity of the signal and by the discrete resolution. However, when used for the analysis of signals coming from a real application, this assumption is not longer valid. The effect of the signal

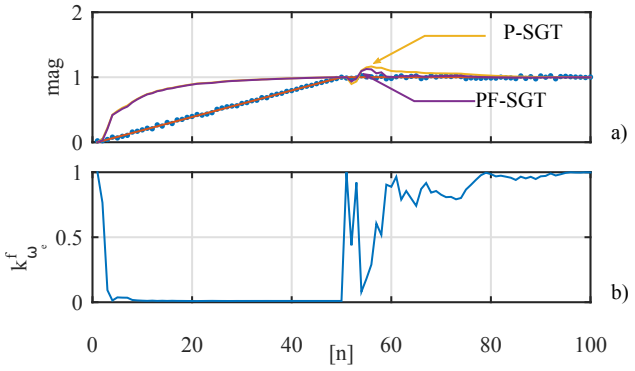

Fig. 5. Proposed fusion mechanism. a) evolution of the module. b) evolution of the gain. $g_{h\omega_e} = 5$, $max(\triangle X^{sgt}_{h\omega_e}) = 1.1$

being not periodic, together with the discrete resolution, will cause spectral leakage, affecting both the phase and magnitude of the estimated components. Often, windowing techniques (both in time and frequency domain) are applied in order to reduce the impact. Unfortunately, the procedure also affects the magnitude and the phase of the extracted components and additional compensation is needed. A different approach is to optimize the parameters for the calculation by adjusting the number of needed samples (200 by default in our implementation) depending on the fundamental frequency, so a complete number of cycles is acquired at each processing window. For this paper, and considering that only the harmonics of the fundamental frequency needs to be isolated, an even simpler approach has been used by selecting a coarse spectral resolution of $50Hz$. This avoids the spectral leakage when deviations from the fundamental frequency appears, at the cost of any other disturbance signal falling within the band of $[25 - 75]Hz$ to be affecting the estimation.

C. Magnitude estimation errors due to the LSE algorithm

The use of the proposed LSE method over a N-length window could affect to the magnitude estimation depending on the sample where the disturbance occurs ($0 < n < N-1$). This is due to the fact that the same slope is assumed over the whole LSE period. This will lead to magnitude estimation errors if any change in the signal magnitude occurs during the LSE calculation period.

In order to test the behavior of the LSE method, Fig. 6 shows the magnitude error when the sample at witch the disturbance happens is continuously varied from 0 to N=200. Different disturbances are considered: a 0.4 p.u. magnitude step, a frequency step from 49 to 51Hz and a phase jump of 60 deg. Two different signals are shown in each graphic: the mean value of the magnitude error over two 200 samples periods is shown in blue color, wheres the magnitude error at the end of the first period is shown in red. As it can be observed, magnitude and phase jumps both affect to the magnitude estimation depending on the sample when they occur.

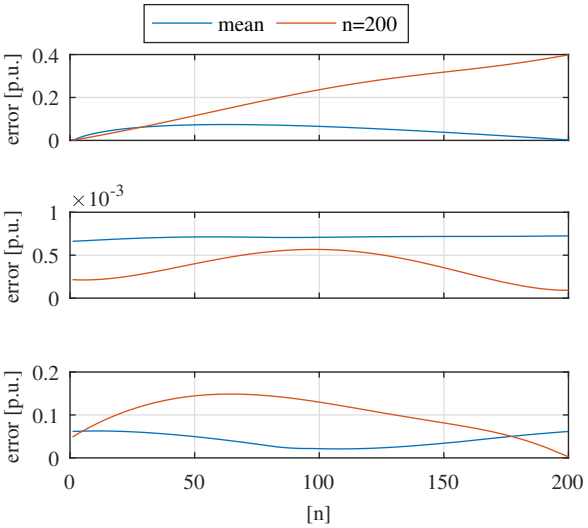

Fig. 6. Effect on the magnitude estimation when the disturbance occurs along the N-length window: a) Magnitude step (0.4 p.u.), b) Frequency Step (2 Hz.) c) Phase Jump (60 deg).

In order to deal with these unwanted errors, what is proposed here is to restart the LSE calculation by looking for a noticeable variation in the estimated magnitude between two consecutive LSE samples, as shown in (4). A threshold (M_{th}) of a 15% of the fundamental positive-sequence magnitude has been selected.

$$\left|X_{\omega_e}^{p-sgt}(n) - X_{\omega_e}^{p-sgt}(n-1)\right| > M_{th} \tag{4}$$

D. Phase-jump detection and magnitude correction

An adverse effect that noticeably affects to the magnitude and frequency estimation is the occurrence of a phase jump. This subsection shows a basic technique that detects a phase jump and corrects its effects in the estimated magnitude. The main working principle of this technique is to check if the phase difference between the actual phase angle estimation and the previous one falls inside the grid code. An acceptable frequency deviation from the nominal value has been selected to be $\omega_{err} = 2 \cdot 2\pi$rad/s. Thus, the phase difference between the actual phase estimation and the previous one (P_s in (5)) should fall inside the phase advance defined by (5), being T_s the sampling time. Thus, if a phase jump is detected, the magnitude estimation at the previous sample is used. Note that a low-pass version of the voltage complex vector could be used, but this solution requires more computational effort at no extra advantage. Fig. 7 shows the proposed correction mechanism compared to the magnitude variation before the compensation.

$$(\omega_e - \omega_{err}) \cdot T_s < P_s < (\omega_e + \omega_{err}) \cdot T_s \tag{5}$$

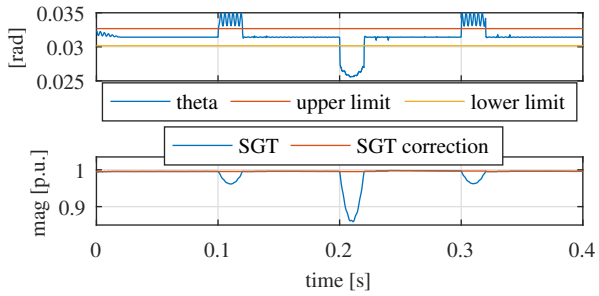

Fig. 7. System evaluation. Compensation of magnitude estimation during a phase-jump.

III. System Evaluation

The initial evaluation of the proposed sequence estimator has been done using a programmable voltage source (2210 TC-ACS-50-480-400 from Regatron) to create the different grid conditions. Different steps at the magnitude, phase and frequency of the signal are considered as well as the behavior with and without additional harmonic content. The data is acquired by an scope at $1Ms/s$ and later down-sampled to $10kHz$. The down-sampled signal is processed in Matlab/Simulink using a real-time implementation.

The results for the tracked grid voltage's magnitude and phase using the PF-SGT are shown in Fig 8 and 9. The different events at the source signal are repeated twice. During the first interval ($t = 0 - 1.2s$), no harmonics were included. At the second part, the harmonics indicated at Table I are considered. Moreover, starting at $t = 1.5s$, a dc offset is included at the output of the voltage sensors. Dc-offset values are $V_u = 10V, V_v = 5V, V_w = -5V$. The events are scheduled as follows: 1) **Magnitude**. At $t = 0.8s$ and $t = 0.9s$ it changes to 0.8 and 1.2 p.u. The same change is observed at $t = 1.98s$ and $t = 2.08s$. 2) **Frequency**. At $t = 0.2s$ and $t = 0.3s$, the rated $50Hz$ frequency is changed to 49 and 51Hz respectively. The same is done $t = 1.38s$ and $t = 1.48s$. 3) **Phase**. At $t = 0.5, t = 0.6, t = 0.7s$ phase jumps of $30, -60, 30$deg. are induced. Same pattern is observed at $t = 1.68, 1.78, 1.88s$. At the graph, the behavior of the proposed method is tested compared to the DSOGI implementation. The tuning of the DSOGI has been done according to the optimal parameters indicated by its authors [9]. As it can be seen, the proposed method shows a better immunity to harmonics and faster response to the considered changes with the exception of the phase change at $t = 0.6$ and $1.78s$. This is due to the correction explained in (5) not being considered for the initial evaluation. It is special remarkable the improvement of the proposed method when DC components are considered. Finally, the compared experimental results for the dynamics of the closed-loop current control using the DSOGI and the proposed PF-SGT method are shown in Fig. 10. For the initial evaluation of the method, the closed-loop current control of a three phase power converter connected to the grid has been used. The current control has been implemented at the synchronous reference frame and different current references,

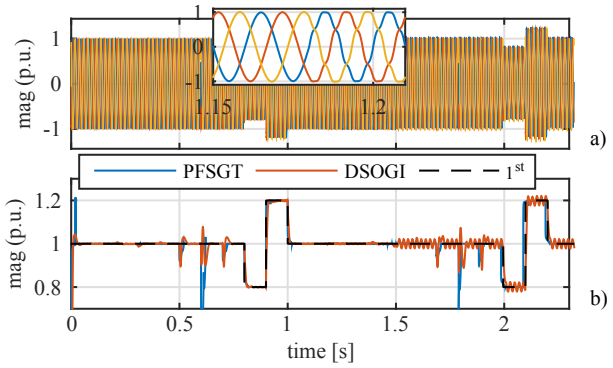

Fig. 8. System evaluation. Comparison of the PF-SGT method with respect to the ideal 1^{st} harmonic and the DSOGI implementation. a) evolution of time domain waveforms, b) evolution of the module estimation.

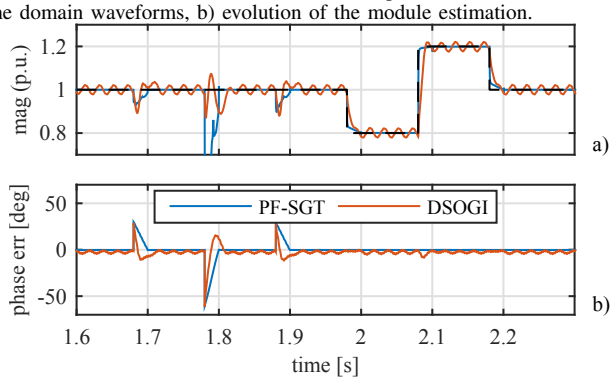

Fig. 9. System evaluation. Detail on the comparison of the PF-SGT method with respect to the ideal 1^{st} harmonic and the DSOGI implementation. a) module, b) phase.

both at the d and q axis were commanded. The grid voltage was acquired as previously explained and the downsampled voltage data was used in a real-time Simulink simulation. The same sequence than for the open-loop results shown in Fig. 8 has been used. The relevant parameters for the setup are: filter values: $L = 5mH, R = 0.2\Omega$, switching frequency $f_{sw} = 10kHz$, current control bandwidth $20Hz$. As clearly shown, the proposed method shows a better transient

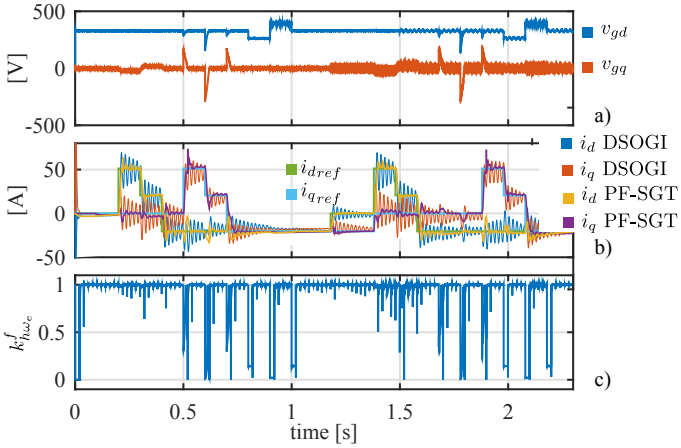

Fig. 10. System evaluation. Close loop comparison between the DSOGI and the proposed PF-SGT methods. a) grid voltages, b) grid currents, c) adaptive fusion gain for the PF-SGT method.

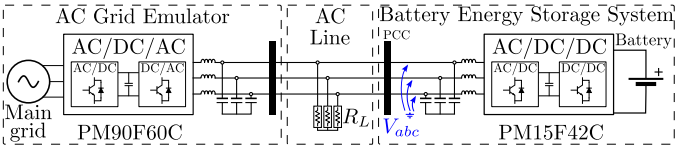

Fig. 11. Setup used for the experimental validation. Two converters are coupled together, PM90F60C unit is used to create the vayring grid conditions and PM15F42C runs the proposed estimation method.

response and harmonic rejection capabilities than the DSOGI alternative. Moreover, the bandwidth was set to such a low value in order to keep stable the DSOGI-based current control.

IV. Experimental Results

For this paper, the evaluation of the proposed sequence estimator is done using the experimental grid shown in Fig. 11. The setup is composed by Triphase power modules PM15F42C and PM90F60C, and a set of passive loads. The module PM90F60C is used as a grid voltage emulator. It creates the different grid scenarios, modifying the magnitude, phase, frequency and harmonic content of the voltage signal. The module PM15F42C is integrated in the system operating as a constant power controlled battery energy storage system. The proposed algorithms are processed online in the PM15F42C control unit using the voltage measurements at the point of common coupling (PCC). The experimental results use the DSOGI algorithm as the base case for the comparison.

A. Variation of grid voltage magnitude

Variations of grid voltage magnitude from 1 to 0.8 p.u. at $t = 0.1$s and from 0.8 to 1.15 p.u. at $t = 0.2$ are considered. Results both without and with $h_5 = 5\%$, $h_7 = 5\%$ additional harmonics are shown in Fig. 12 and Fig. 13 respectively. As shown, the proposed method have a faster dynamic response as well as higher harmonic robustness, both for the magnitude and the phase estimation.

B. Variation of grid voltage frequency

Variations of grid voltage frequency from 50 to 49 Hz. at $t = 0.1$s and from 49 to 51 Hz. at $t = 0.2$ are considered. Results both without and with $h_5 = 5\%$, $h_7 = 5\%$ additional harmonics are shown in Fig. 14 and Fig. 15 respectively. As shown, the proposed method have a better magnitude response. However, an steady state error in the phase appears with the proposed method. The reason is the considered frequency resolution. As explained before, a frequency resolution of 50 Hz. has been selected for this work. This implies that any deviation smaller than 50Hz can not be measured and the difference between the real grid frequency and the fundamental harmonic is directly coupled to a phase error. However, the maximum possible error under the maximum considered frequency deviation is bounded and given by the expression (6). Where $\max(\omega_{err})$ is the maximum frequency error and f_e the grid frequency in Hz. The maximum frequency error depends on the frequency resolution and the maximum admissible grid

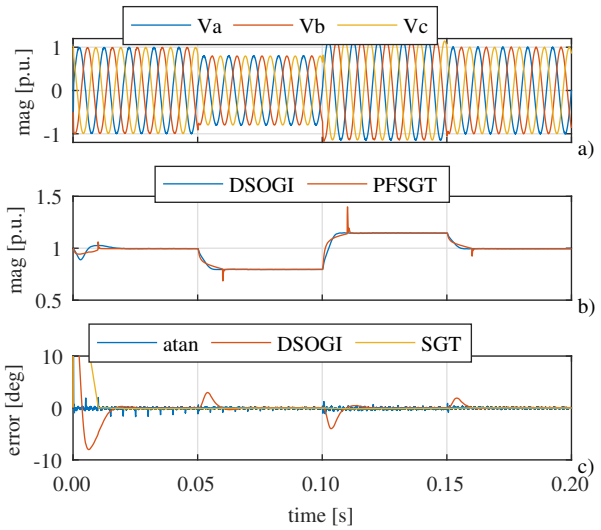

Fig. 12. Experimental results. Comparison between the DSOGI and the proposed PF-SGT methods for a magnitude step change. No harmonics are injected. From top to bottom: a) grid voltages, b) grid voltage magnitude, c) grid voltage phase error.

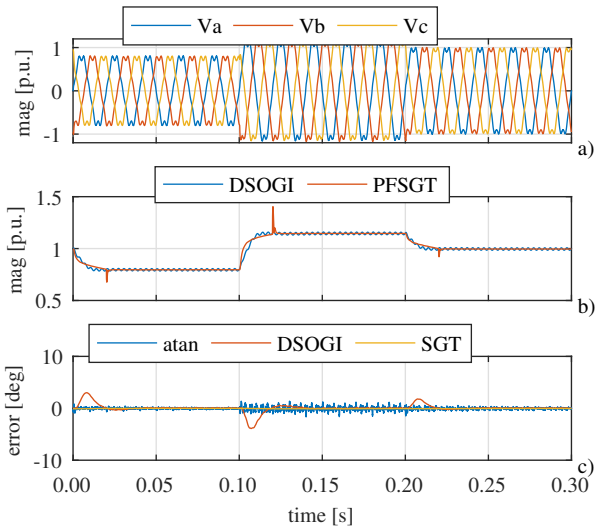

Fig. 13. Experimental results. Comparison between the DSOGI and the proposed PF-SGT methods for a magnitude step change. Harmonics as listed in Table I are injected. From top to bottom: a) grid voltages, b) grid voltage magnitude, c) grid voltage phase error.

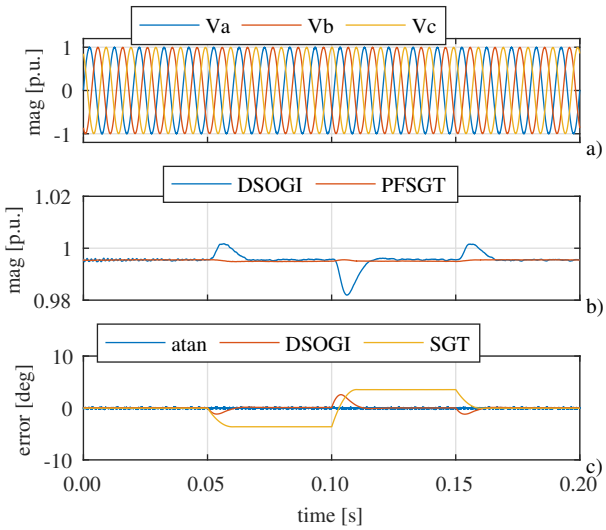

Fig. 14. Experimental results. Comparison between the DSOGI and the proposed PF-SGT methods for a frequency step change. No harmonics are injected. From top to bottom: a) grid voltages, b) grid voltage magnitude, c) grid voltage phase error.

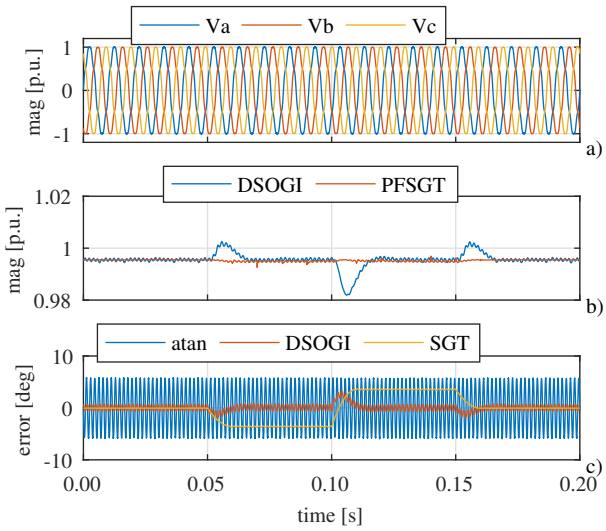

Fig. 15. Experimental results. Comparison between the DSOGI and the proposed PF-SGT methods for a frequency step change. Harmonics as listed in Table I are injected. From top to bottom: a) grid voltages, b) grid voltage magnitude, c) grid voltage phase error.

frequency deviation. For the values considered at this paper, the error is bounded to a maximum of 3.6deg.

$$\max \theta_{err} = \frac{\max(\omega_{err})2\pi}{f_e} \cdot \frac{180}{2\pi} \tag{6}$$

C. Variation of grid voltage phase

Variations of grid voltage phase from 0 to 30 deg. at $t = 0.05$s, from 30 to -30 deg. at $t = 0.1$ and from -30 to 0 at $t = 0.15$s are considered. Results both without and with $h_5 = 5\%$, $h_7 = 5\%$ additional harmonics are shown in Fig. 16 and Fig. 17 respectively. As shown, the proposed method have a similar results compared to DSOGI when no additional harmonics are considered and a clearly improve response under harmonic conditions.

V. Conclusion

This paper has introduced a new predictive estimation technique for grid-tied converters based on a frequency-based method. To the author's best knowledge, the proposed method using a modification of the Sliding Goertzel Transformation (SGT) which includes a predictive modification has not been used before for grid phase tracking in power converters. The proposed PF-SGT method has been evaluated with respect to

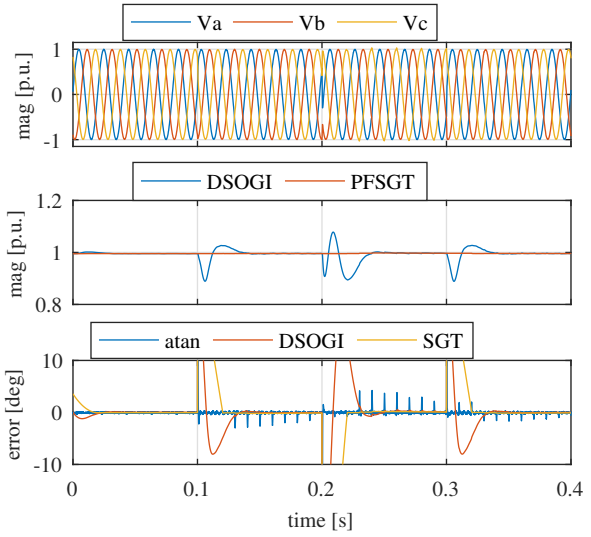

Fig. 16. Experimental results. Comparison between the DSOGI and the proposed PF-SGT methods for a phase step change. No harmonics are injected. From top to bottom: a) grid voltages, b) grid voltage magnitude, c) grid voltage phase error.

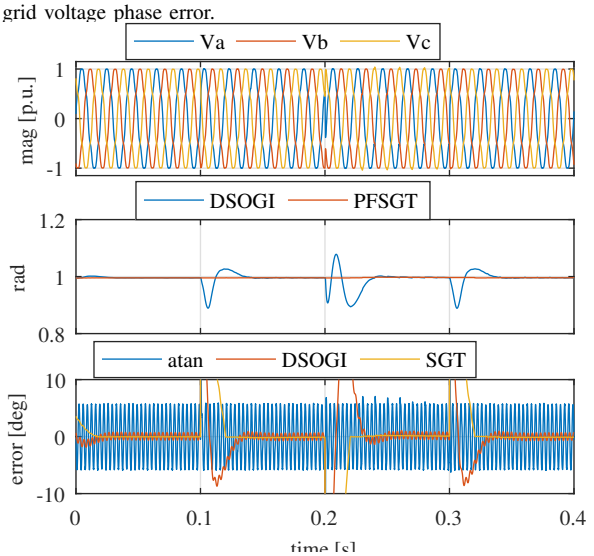

Fig. 17. Experimental results. Comparison between the DSOGI and the proposed PF-SGT methods for a phase step change. Harmonics as listed in Table I are injected. From top to bottom: a) grid voltages, b) grid voltage magnitude, c) grid voltage phase error.

a consolidated alternative, the DSOGI, showing a superior performance in terms of dynamic response and disturbance rejection. It is particular remarkable the immunity to DC offsets as well as to changes at the grid frequency. The proposed algorithm has been validated by both simulation and experimental results. The impact of the phase estimation and harmonic decoupling in a closed-loop current control implementation has also been evaluated, being the proposed PF-SGT an important improvement over the DSOGI method.

REFERENCES

[1] C. Blanco, D. Reigosa, J. C. Vasquez, J. M. Guerrero, and F. Briz, "Virtual admittance loop for voltage harmonic compensation in microgrids," *IEEE Transactions on Industry Applications*, vol. 52, no. 4, pp. 3348–3356, July 2016.

[2] J. W. Simpson-Porco, Q. Shafiee, F. Dörfler, J. C. Vasquez, J. M. Guerrero, and F. Bullo, "Secondary frequency and voltage control of islanded microgrids via distributed averaging," *IEEE Transactions on Industrial Electronics*, vol. 62, no. 11, pp. 7025–7038, Nov 2015.

[3] E. Twining and D. G. Holmes, "Grid current regulation of a three-phase voltage source inverter with an lcl input filter," *IEEE Transactions on Power Electronics*, vol. 18, no. 3, pp. 888–895, May 2003.

[4] S. Yang, Q. Lei, F. Z. Peng, and Z. Qian, "A robust control scheme for grid-connected voltage-source inverters," *IEEE Transactions on Industrial Electronics*, vol. 58, no. 1, pp. 202–212, Jan 2011.

[5] J. C. Vasquez, J. M. Guerrero, M. Savaghebi, J. Eloy-Garcia, and R. Teodorescu, "Modeling, analysis, and design of stationary-reference-frame droop-controlled parallel three-phase voltage source inverters," *IEEE Transactions on Industrial Electronics*, vol. 60, no. 4, pp. 1271–1280, April 2013.

[6] S. Golestan, J. M. Guerrero, and J. C. Vasquez, "Three-phase plls: A review of recent advances," *IEEE Transactions on Power Electronics*, vol. 32, no. 3, pp. 1894–1907, March 2017.

[7] F. D. Freijedo, J. Doval-Gandoy, O. Lopez, and E. Acha, "A generic open-loop algorithm for three-phase grid voltage/current synchronization with particular reference to phase, frequency, and amplitude estimation," *IEEE Transactions on Power Electronics*, vol. 24, no. 1, pp. 94–107, Jan 2009.

[8] S. Golestan, A. Vidal, A. G. Yepes, J. M. Guerrero, J. C. Vasquez, and J. Doval-Gandoy, "A true open-loop synchronization technique," *IEEE Transactions on Industrial Informatics*, vol. 12, no. 3, pp. 1093–1103, June 2016.

[9] P. Rodriguez, A. Luna, M. Ciobotaru, R. Teodorescu, and F. Blaabjerg, "Advanced grid synchronization system for power converters under unbalanced and distorted operating conditions," in *IECON 2006 - 32nd Annual Conference on IEEE Industrial Electronics*, Nov 2006, pp. 5173–5178.

[10] P. Rodriguez, R. Teodorescu, I. Candela, A. Timbus, M. Liserre, and F. Blaabjerg, "New positive-sequence voltage detector for grid synchronization of power converters under faulty grid conditions," in *2006 37th IEEE Power Electronics Specialists Conference*, June 2006, pp. 1–7.

[11] A. M. Gole and V. K. Sood, "A static compensator model for use with electromagnetic transients simulation programs," *IEEE Transactions on Power Delivery*, vol. 5, no. 3, pp. 1398–1407, Jul 1990.

[12] C. Blanco, D. Reigosa, F. Briz, and J. M. Guerrero, "Synchronization in highly distorted three-phase grids using selective notch filters," in *2013 IEEE Energy Conversion Congress and Exposition*, Sept 2013, pp. 2641–2648.

[13] X. Guo, W. Wu, and Z. Chen, "Multiple-complex coefficient-filter-based phase-locked loop and synchronization technique for three-phase grid-interfaced converters in distributed utility networks," *Industrial Electronics, IEEE Transactions on*, vol. 58, no. 4, pp. 1194–1204, April 2011.

[14] C. Blanco, D. Reigosa, F. Briz, J. M. Guerrero, and P. Garcia, "Grid synchronization of three-phase converters using cascaded complex vector filter pll," in *2012 IEEE Energy Conversion Congress and Exposition (ECCE)*, Sept 2012, pp. 196–203.

[15] F. D. Freijedo, A. G. Yepes, O. Lopez, A. Vidal, and J. Doval-Gandoy, "Three-phase plls with fast postfault retracking and steady-state rejection of voltage unbalance and harmonics by means of lead compensation," *IEEE Transactions on Power Electronics*, vol. 26, no. 1, pp. 85–97, Jan 2011.

[16] S. Golestan, J. M. Guerrero, A. Vidal, A. G. Yepes, and J. Doval-Gandoy, "Pll with maf-based prefiltering stage: Small-signal modeling and performance enhancement," *IEEE Transactions on Power Electronics*, vol. 31, no. 6, pp. 4013–4019, June 2016.

[17] C. Blanco, D. Reigosa, F. Briz, and J. M. Guerrero, "Quadrature signal generator based on all-pass filter for single-phase synchronization," in *2014 IEEE Energy Conversion Congress and Exposition (ECCE)*, Sept 2014, pp. 2655–2662.

[18] E. Jacobsen and R. Lyons, "An update to the sliding dft," *IEEE Signal Processing Magazine*, vol. 21, no. 1, pp. 110–111, Jan 2004.

[19] G. Goertzel, "An Algorithm for the Evaluation of Finite Trigonometric Series," *The American Mathematical Monthly*, vol. 65, no. 1, pp. 34–35, 1958.